



# Assessment of the partitioning capacity of high abundant proteins in human cerebrospinal fluid using affinity and immunoaffinity subtraction spin columns

Magnus Wetterhall, Aida Zuberovic, Jörg Hanrieder, Jonas Bergquist\*

Department of Physical and Analytical Chemistry, Analytical Chemistry, Uppsala University, Uppsala, Sweden

## ARTICLE INFO

### Article history:

Received 10 February 2010

Accepted 1 April 2010

Available online 13 April 2010

### Keywords:

Cerebrospinal fluid (CSF)  
Mass spectrometry (MS)  
Proteomics  
Immunoaffinity subtraction  
Protein fractionation  
iTRAQ quantification

## ABSTRACT

The performance of three different affinity and immunoaffinity subtraction spin columns was investigated for the removal of the most abundant proteins in human cerebrospinal fluid (CSF). A pool of human CSF was processed with the spin columns and both the bound and flow through fractions were compared with each other and with intact CSF using 1D gel electrophoresis and nanoLC–MALDI-TOF/TOF-MS analysis. MASCOT MS/MS ionscores were compared before and after processing with the columns. The non-specific co-removal of proteins bound to the high abundant proteins, so called “sponge effect” was also examined for each spin column. The reproducibility of one of the spin columns, ProteomeLab IgY-12 proteome partitioning spin column, was further investigated by isobaric tags for relative and absolute quantification (iTRAQ) labeling and MS/MS analysis. Overall, 173 unique proteins were identified on a 95% MudPIT confidence scoring level. For all three spin columns, the number of proteins identified and their MASCOT scores were increased up to 10 times. The largest degree of non-specific protein removal was observed for a purely affinity based albumin removal column, where 28 other proteins also were present. The ProteomeLab IgY-12 proteome partitioning spin column showed very high reproducibility when combined with iTRAQ labeling and MS/MS analysis. The combined relative standard deviation (R.S.D.) for the high abundant protein removal, iTRAQ labeling and nanoLC–MALDI-TOF/TOF-MS analysis was less than 17.5%.

© 2010 Elsevier B.V. All rights reserved.

## 1. Introduction

In recent years, a lot of emphasis has been put on the proteomic analysis of cerebrospinal fluid (CSF), especially in the quest to find biomarkers for neurological disorders [1–9]. CSF is of great clinical interest due to the continuous contact and exchange with the central nervous system (CNS). The hypothesis is that changes in the CNS, caused by the disease, should be reflected in the CSF and therefore of high interest to measure. The greatest challenges in proteomic analysis of CSF are the complexity, diversity and large dynamic range of concentration of the proteins and peptides present in the sample. The total protein concentration in CSF is rather low (0.2–0.8 mg/mL) compared to plasma (50–80 mg/mL) and the majority of the proteins in CSF are believed to originate

from plasma through the blood–brain barrier [5,10,11]. A few high abundant proteins constitute the greater part of the total protein concentration, thus limiting the sample loading and detection capabilities for low abundant proteins. For example, albumin represents approximately 60% of the total protein content in CSF and the 10 most common proteins in CSF constitute more than 80% of the total protein composition [5]. It is believed that potential biomarkers secreted in biofluids would be present at very low concentrations [12]. Therefore, there is a great need to remove the high abundant proteins to facilitate the detection of these low abundant potential biomarkers. Several protein removal, fractionation and concentration strategies have been explored for CSF including solvent depletion schemes [2,13], ultrafiltration [14–16], in-solution isoelectric focusing (IEF) [17–19], reversed phase solid phase extraction [20], peptide binding ligands [21], affinity [22–26] and antibody based chromatography [15,23,27–35]. All these techniques have shown an improvement in the number of proteins identified in CSF compared to analyzing the intact sample. Of the above mentioned techniques, the immunoaffinity based ones have shown the best specificity in the removal of targeted high abundant proteins. However, one should be aware that the subtraction of transport proteins, such as albumin and transferrin, can lead to co-removal of low abundant proteins bound to the carrier proteins [36,37]. The aim of this study was to compare the performance

*Abbreviations:* ACN, acetonitrile; B, bound fraction; CSF, cerebrospinal fluid; DTT, dithiothreitol; HAc, acetic acid; FT, flow through fraction; IAA, iodoacetamide; iTRAQ, isobaric tags for relative and absolute quantification; MALDI, matrix assisted laser desorption ionization; MS, mass spectrometry; TFA, trifluoroacetic acid; TOF, time-of-flight.

\* Corresponding author at: Department of Physical and Analytical Chemistry, Analytical Chemistry, Uppsala University, P.O. Box 599, SE-751 24 Uppsala, Sweden. Tel.: +46 18 4713675; fax: +46 18 4713692.

E-mail address: [jonas.bergquist@kemi.uu.se](mailto:jonas.bergquist@kemi.uu.se) (J. Bergquist).

for three different affinity and immunoaffinity based spin columns for the partitioning of the most abundant proteins in human CSF by analyzing both the bound and flow through protein fractions. These spin columns were designed for human plasma applications, as there is still today no kit primarily intended for human CSF fractionation. However, since the protein composition is very similar in both body fluids, the columns can readily be used for the processing of CSF. The protein partitioning performance of the spin columns was evaluated by 1D gel electrophoresis and liquid chromatography in combination with matrix assisted laser desorption ionization time-of-flight tandem mass spectrometry (LC–MALDI-TOF/TOF-MS). Furthermore, the reproducibility for one of the columns was more thoroughly investigated in combination with the popular iTRAQ™ labeling technique [38] for quantitative mass spectrometry (MS) analysis of complex protein samples. Stable isotopic labeling, such as isobaric tags for relative and absolute quantification (iTRAQ), has virtually boomed the application of quantitative MS in proteomic research. The major reasons for this are the multiplexing possibilities which in turn imply comparative quantification under identical conditions and a higher sample throughput. Multiplexing is a very attractive feature in biomarker screening studies and differential diagnosis where healthy and disease states are quantitatively compared. The use of affinity and immunoaffinity fractionation in combination with stable isotopic labeling and MS detection is today the method of choice for such proteomic studies.

## 2. Experimental

### 2.1. Chemicals and reagents

Acetonitrile (ACN), acetic acid (HAc) and ammonium-dihydrogen-phosphate ( $\text{NH}_4\text{H}_2\text{PO}_4$ ) were obtained from Merck (Darmstadt, Germany). Acetone and trifluoroacetic acid (TFA) were purchased from Sigma–Aldrich (St. Louis, MO, USA). For tryptic digestion, urea, ammonium bicarbonate ( $\text{NH}_4\text{HCO}_3$ ), iodoacetamide (IAA) and dithiothreitol (DTT) were obtained from Sigma and trypsin (sequence-grade from bovine pancreas (1418475); Roche diagnostics, Basel, Switzerland) was used. The water was purified with a Milli-Q (Millipore, Bedford, MA, USA) purification system.

### 2.2. Samples

Human cerebrospinal fluid used was taken from a pool consisting of >200 individual CSF samples drawn from patients in the age of 16–65 years. The majority of the samples were collected by lumbar puncture during epidural anesthetics procedures and none of the patients showed signs of neurological or psychiatric disorders. Routine CSF analysis revealed no signs of inflammation or damage to the blood–brain barrier function. The study was approved by the local Human Ethics Committee. The pooled CSF sample was stored at  $-80^\circ\text{C}$  until preparation and analysis.

### 2.3. Sample preparation

A schematic overview of the experimental set-up is shown in Fig. 1. Multiple aliquots of 100  $\mu\text{L}$ , 250  $\mu\text{L}$ , 500  $\mu\text{L}$  and 1000  $\mu\text{L}$  of the pooled CSF were centrifuged to dryness using a Speedvac system ISS110 (Thermo Scientific, Waltham, MA, USA). For high abundant protein fractionation, three different affinity/antibody spin column kits were used. All three kits are designed to process 10–15  $\mu\text{L}$  of human plasma samples. The Montage Albumin Depletion Kit (Millipore) removes more than 50% of albumin and has less than 14% non-specific removal of proteins bound to albumin. The

ProteomeLab™ IgY-12 proteome partitioning kit (Beckman Coulter, Fullerton, CA, USA) removes 12 of the most common plasma proteins and the ProteoPrep® 20 Plasma Immunodepletion Kit (Sigma) is designed for removal of 20 of the most abundant proteins. The targeted proteins for each kit are listed in Table 1. The dry CSF pellets were redissolved in 500  $\mu\text{L}$  sample buffer (supplied with the kit) and treated according to the protocols provided by the manufacturers. Both the flow through (FT) and bound (B) fractions of CSF from each kit were collected. The FT fractions from each kit were centrifuged to dryness prior to 1D gel electrophoresis (Section 2.6) or enzymatic digestion (Section 2.5) followed by nanoLC–MALDI-TOF/TOF-MS analysis (Section 2.7). The bound fractions from each kit contained different detergents, which are not compatible with the downstream LC–MS analysis. Thus, these fractions were first precipitated with acetone and then analyzed by 1D gel electrophoresis (Section 2.6) or enzymatic digestion and nanoLC–MALDI-TOF/TOF-MS (Sections 2.5 and 2.7). The acetone precipitation was conducted by first adding six sample volumes of ice cold acetone. The samples were left in  $-20^\circ\text{C}$  over night and then spun at  $10\,000 \times g$  for 30 min at  $4^\circ\text{C}$  using a Sigma 2K15 centrifuge. The supernatant was removed and six sample volumes of ice cold 50% acetone were added. The samples were briefly vortexed and spun again at  $10\,000 \times g$  for 30 min at  $4^\circ\text{C}$ . The supernatant was discarded and the protein pellets were dried at ambient temperature prior to further processing and analyses. Finally, aliquots of 100  $\mu\text{L}$ , 250  $\mu\text{L}$ , 500  $\mu\text{L}$  and 1000  $\mu\text{L}$  of non-depleted CSF were also dried and analyzed with 1D gel electrophoresis (Section 2.6) and nanoLC–MALDI-TOF/TOF-MS (Sections 2.5 and 2.7) as control comparison.

### 2.4. Bradford protein assay

The total protein content was estimated on the start CSF and aliquots taken throughout the sample preparation with Bradford Coomassie® Brilliant Blue G-250 protein assay using bovine serum albumin (BSA) as standard (Bio-Rad, Hercules CA, USA). The absorbance was measured using a Bio-Rad Model 680 microplate reader at 595 nm.

### 2.5. Protein digestion and desalting

The dry pellets from non-processed CSF and the corresponding dried FT fractions and B fractions from each affinity/antibody kit were redissolved in 100  $\mu\text{L}$  8 M urea, 0.4 M  $\text{NH}_4\text{HCO}_3$  after which 10  $\mu\text{L}$  of 45 mM DTT was added and the samples were incubated at  $50^\circ\text{C}$  for 15 min to reduce the disulfide bridges between the cysteines. After cooling to room temperature, 10  $\mu\text{L}$  of 100 mM IAA was added and the samples were incubated for 15 min at room temperature in darkness to irreversibly carbamidomethylate the cysteines. Finally, trypsin 100  $\mu\text{g}$  dissolved in 1 mL 50 mM  $\text{NH}_4\text{HCO}_3$  was added to the samples to yield a 2% (w/w) trypsin/protein concentration and the samples were digested over night at  $37^\circ\text{C}$ . A volume of 20  $\mu\text{L}$  of the tryptically digested sample was desalted on a ZipTip® C18 column (Millipore) using a procedure described by Bergquist et al. [39]. The tip was first wetted in  $5 \times 10 \mu\text{L}$  of 100% ACN and equilibrated with  $5 \times 10 \mu\text{L}$  1% HAc. The samples were acidified to a concentration of 2.5% HAc, after which the peptides were adsorbed on the media using 20 repeated cycles of sample loading. The tip was washed using  $5 \times 10 \mu\text{L}$  of 1% HAc, and the peptides were eluted in  $2 \times 10 \mu\text{L}$  of 50% ACN, 1% HAc. This procedure was repeated twice for each sample. After the desalting, the eluate was vacuum centrifuged to dryness. The peptides were redissolved in 20  $\mu\text{L}$  of 0.1% TFA prior to nanoLC–MALDI-TOF/TOF-MS analysis.

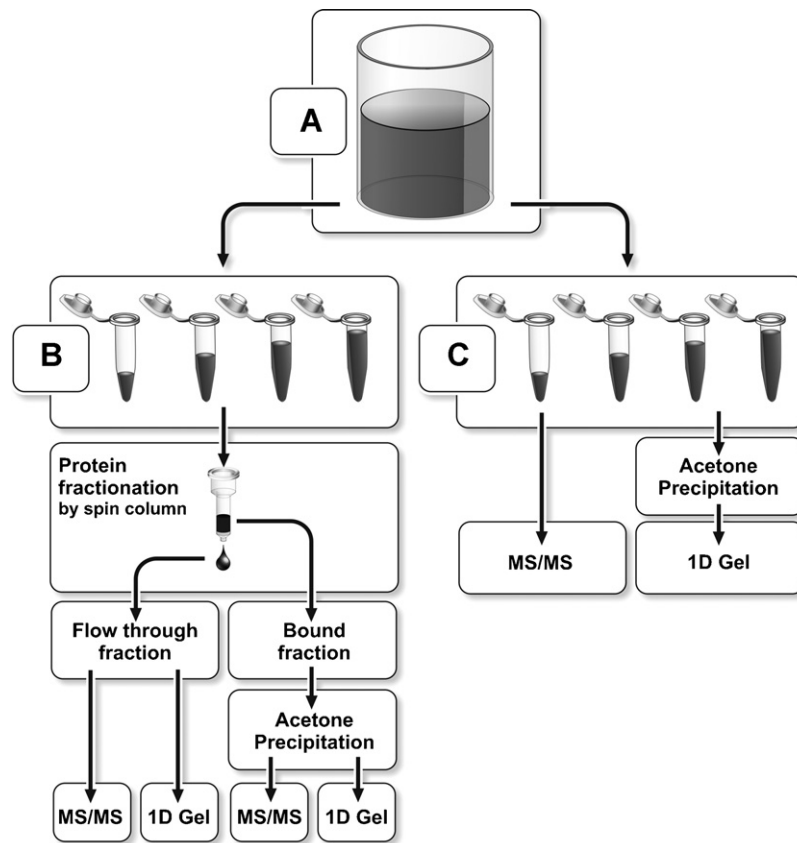


**Fig. 1.** (A) Schematic overview of the experimental set-up for comparing the protein partitioning efficiency for the different subtraction spin columns and non-processed human cerebrospinal fluid (CSF). A large pool of CSF (A) was split into multiple aliquots of 100  $\mu\text{L}$ , 250  $\mu\text{L}$ , 500  $\mu\text{L}$  and 1000  $\mu\text{L}$  for processing with the protein subtraction spin columns (B) or for use as non-processed control CSF (C). The subtraction spin columns yielded a flow through and bound fraction. The flow through fractions were either digested and analyzed by nanoLC–MALDI-TOF/TOF-MS or separated on a 1D gel. The bound fractions were first precipitated by acetone and then either digested and analyzed by nanoLC–MALDI-TOF/TOF-MS or separated on a 1D gel. The non-processed control CSF aliquots were either digested and analyzed by nanoLC–MALDI-TOF/TOF-MS or acetone precipitated and then separated on a 1D gel.

## 2.6. 1D gel electrophoresis

1D gel electrophoresis was performed on the non-depleted CSF, FT fractions and B fractions for each kit to visually examine the depletion efficiency and capacity. The 1D gel electrophoresis was performed with a Criterion XT™ system using precast Criterion XT 26 well 4–12% Bis–Tris gels with XT MOPS running buffer (Bio-Rad). The samples were redissolved in 25  $\mu\text{L}$  XT sample buffer, 55  $\mu\text{L}$  MQ water and 10  $\mu\text{L}$  45 mM DTT. The samples were heated to 95 °C for 5 min, cooled to room temperature and 10  $\mu\text{L}$  100 mM IAA was added. The gels were run at 200 V constant for 60 min (starting current 165–175 mA/gel, final current 60–70 mA/gel). Finally, the gels were visualized by either Coomassie Blue R-250 or Silver Stain Plus™ (Bio-Rad) according to the manufacturer's instructions.

## 2.7. LC–MALDI-TOF/TOF-MS analysis

The reversed phase liquid chromatography separation was performed with a 1100 nanoflow LC system (Agilent Technologies, Waldbronn, Germany), equipped with a fraction collector for direct

fractionations onto a MALDI target plate [40]. A volume of 10  $\mu\text{L}$  digestion products was injected into a 10  $\mu\text{L}$  sample loop. For separating the peptides, a 15 cm  $\times$  180  $\mu\text{m}$ , C18 column (Thermo) with 5  $\mu\text{m}$  particle size and an  $\text{H}_2\text{O}:\text{ACN}:\text{TFA}$  solvent system ( $\text{H}_2\text{O}$ , 0.1% TFA mobile phase [A];  $\text{ACN}$ , 0.1% TFA mobile phase [B]) was used. A flow rate of 2  $\mu\text{L}/\text{min}$  was applied, starting with isocratic elution at 2% B during 20 min, followed by gradient elution from 2% to 8% B during 5 min, then from 8% to 32% B within 86 min, then from 32% to 40% B during 5 min and finally from 40% to 80% B during 1 min. The on-line fractionation onto a MALDI target was performed with four fractions per minute for 96 min within the elution period from 20 min (2% B) and 116 min (40% B) resulting in 384 fractions. For optimal MS results, disposable pre-spotted anchorchip targets (PAC-targets, Bruker Daltonics, Bremen, Germany) were chosen. The targets were washed with 10 mM  $\text{NH}_4\text{H}_2\text{PO}_4/0.1\%$  TFA prior to MALDI-TOF/TOF-MS analysis. Mass data were acquired with an Ultraflex II MALDI-TOF/TOF-MS (Bruker Daltonics) in reflector positive mode. A mass range of 700–4000 Da was analyzed with a sum of 300 shots/spot and 50 shots/position, respectively, in a hexagonal pattern. The laser frequency was set to 100 Hz.

**Table 1**  
Targeted high abundant plasma protein for each spin column kit used in the study.

Montage	ProteomeLab IgY-12	ProteoPrep 20
Albumin	Albumin, IgA, IgG, IgM, $\alpha$ 1-antitrypsin, transferrin, haptoglobin, $\alpha$ 1-acid glycoprotein (orosmucoid), $\alpha$ 2-macroglobulin, Apolipoprotein A-I, Apolipoprotein A-II and Fibrinogen	Albumin, IgA, IgD, IgG, IgM, $\alpha$ 1-antitrypsin, transferrin, haptoglobin, $\alpha$ 1-acid glycoprotein (orosmucoid), $\alpha$ 2-macroglobulin, Apolipoprotein A-I, Apolipoprotein A-II, Fibrinogen, ceruloplasmin, Apolipoprotein B, complement C1q, complement C3, complement C4, plasminogen and prealbumin

MALDI-TOF/TOF tandem MS analysis was performed in post source decay MS/MS mode with 30% increased laser energy to give the fragmentation spectra. Post fragmentation mother ion suppression was applied to deflect the precursor and elevate fragment ion intensity. Peptide monoisotopic signals were analyzed using the FlexAnalysis software provided with the instrument (Bruker Daltonics). The spectra were calibrated externally using the pre-spotted calibrants adjacent to the sample spots. For final protein identification, all collected MS/MS data were run in a comprehensive MS/MS ion search using the MASCOT search engine version 2.2.2 (Matrix Science, London, UK). Acquired MS/MS-spectra were evaluated with the Matrix Science MASCOT database SwissProt version 51.6. The search parameters were set to Taxonomy: Homo sapiens, Enzyme: Trypsin, Fixed modifications: Carbamidomethyl (C), Variable modifications: Oxidation (M), Peptide mass tolerance:  $\pm 50$  ppm, Fragment mass tolerance:  $\pm 0.8$  Da and maximum 1 missed cleavage site. Proteins were considered to be positively matched if at least one MS/MS spectrum fulfilled an individual MASCOT MS/MS MudPIT Ionscore  $> 27$  (significance threshold set to 95% ( $p \leq 0.05$ )).

### 2.8. Sample preparation and iTRAQ labeling

Four 1 mL aliquots of the pooled CSF sample were centrifuged to dryness for processing with the ProteomeLab™ IgY-12 proteome partitioning kit. The dry CSF pellets were redissolved in 500  $\mu$ L modified sample buffer containing 10 mM  $\text{NaH}_2\text{PO}_4/\text{Na}_2\text{HPO}_4$  (pH 7.4) and 150 mM NaCl. A phosphate buffer was used instead of the tris-buffer supplied by the manufacturer since any added primary amines or ammonium salts will affect the following iTRAQ™ labeling efficiency. The redissolved CSF samples were then treated according to the protocol provided by the manufacturer with the exception of using the phosphate buffer instead of the tris-buffer for sample loading and washing. The four obtained FT fractions were centrifuged to dryness and then labeled with the iTRAQ™ 4-plex kit (Applied Biosystems, Foster City, CA, USA) following a slightly changed protocol concerning the denaturing agent. The samples were redissolved in 20  $\mu$ L dissolution buffer, 1  $\mu$ L 1 M urea solution (instead of SDS as suggested in the standard protocol) for protein denaturation. After iTRAQ labeling, equal volumes (90  $\mu$ L) of each of the iTRAQ labeled samples were mixed and dried down under vacuum to remove the added ethanol. The dried sample was redissolved in 2.5% HAC and desalted on a ZipTip® C18 column. The eluate was centrifuged to dryness and then separated by nanoLC, fractionated onto a PAC MALDI target and analyzed by MALDI-TOF/TOF-MS as described previously in Section 2.7. The MASCOT search criteria were changed to: Taxonomy: Homo sapiens, Enzyme: Trypsin, Variable modifications: Oxidation (M), Peptide mass tolerance:  $\pm 50$  ppm, Fragment mass tolerance:  $\pm 0.8$  Da, maximum 1 missed cleavage site and Quantitation: iTRAQ 4-plex.

## 3. Results and discussion

### 3.1. 1D gel electrophoresis of fractionated CSF

All three investigated affinity/antibody kits are designed for the processing of 10–15  $\mu$ L of human plasma. Although the protein concentration in human CSF is at least 100 times less than that for plasma, the major proteins and their relative abundance found in both fluids are very similar [5]. This means that comparatively large CSF volumes (at least 1 mL) can be processed with the plasma spin columns with retained protein removal capacity. Volumes of up to 1 mL of CSF were processed with each spin column and separated by 1D gel electrophoresis to visually examine the working

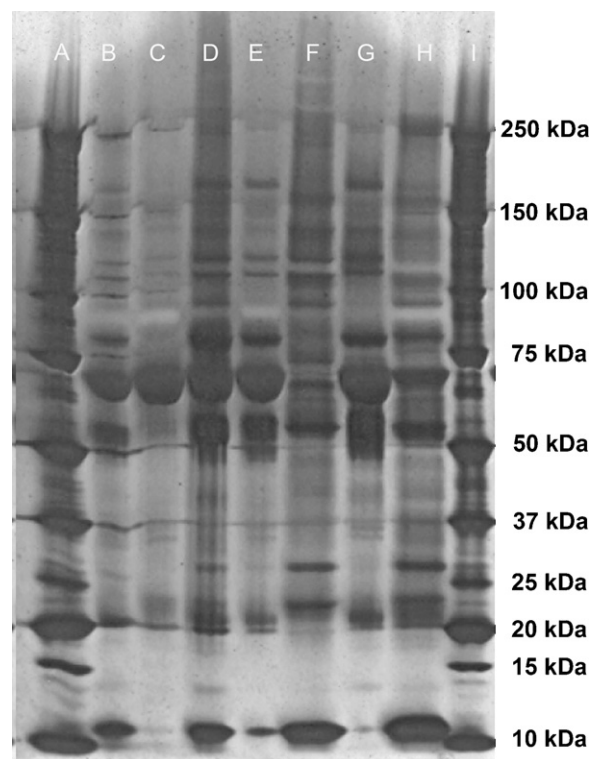


**Fig. 2.** 1D gel of 1 mL intact CSF and the bound and flow through fractions of 1 mL processed CSF from each spin column. The lanes are: A and I: molecular weight markers, B: 1 mL intact CSF, C: Montage bound fraction of 1 mL CSF, D: Montage flow through fraction of 1 mL CSF, E: ProteomeLab IgY-12 bound fraction of 1 mL CSF, F: ProteomeLab IgY-12 flow through fraction of 1 mL CSF, G: ProteoPrep 20 bound fraction of 1 mL CSF and H: ProteoPrep 20 flow through fraction of 1 mL CSF.

range for CSF volumes. Fig. 2 shows the 1D gel electrophoresis separation of intact CSF and the bound and flow through fractions of 1 mL CSF using the different columns. It can clearly be seen that even though albumin is not completely removed, the sample loading of the less abundant proteins has dramatically increased. For all three spin columns, the number of protein bands in the FT fractions (lane D, F and H) are substantially greater than for intact CSF (lane B). The so called “albumin sponge effect” can also be observed in lane C; Montage bound fraction, showing a rather large co-removal of other proteins than the targeted albumin. This unspecific protein removal has also been reported by the manufacturer. Yet, it is important to be aware of this when any comparative or differential proteomic studies are performed, as the results may be biased. The results from the 1D gel shows that volumes of at least up to 1 mL of CSF readily can be processed with spin columns and still obtain satisfactory fractionation results.

### 3.2. nanoLC–MALDI-TOF/TOF-MS analysis

To further evaluate the fractionation efficiency of the target proteins, the sample loading increase of the remaining medium–low abundant proteins and the effect of the observed albumin sponge effect, nanoLC–MALDI-TOF/TOF-MS analysis was performed on 1 mL intact CSF and the FT and B fractions of 1 mL CSF for each spin column. Overall, 173 unique proteins were identified in the CSF as listed in Table 2. For the intact CSF, 91 unique proteins were identified, 128 proteins for the Montage spin column, 123 proteins for the ProteomeLab IgY-12 spin column and 104 proteins for the ProteoPrep 20 spin column. The MASCOT scores before and after sample preparation for the matched proteins are visualized in Fig. 3. Again, in all three cases the MASCOT scores for the medium and low

**Table 2**  
 Proteins identified on 95% MudPIT confidence level in 1 mL intact CSF and the flow through (FT) and bound (B) fractions of 1 mL CSF for each spin column by nanoLC–MALDI-TOF/TOF-MS analysis. The protein classification, molecular weight (MW) and protein function are as given by the Uniprot database.

Protein name	Uniprot entry	Uniprot Acc.	MW	Function	Intact CSF		Montage FT		Montage B		IgY-12 FT		IgY-12 B		PP-20 FT		PP-20 B		
					Score	Pep.	Score	Pep.	Score	Pep.	Score	Pep.	Score	Pep.	Score	Pep.	Score	Pep.	
<i>Transport/binding</i>																			
Serum albumin	ALBU_HUMAN	P02768	71317	Transport	4043	59	3625	59	3255	70	292	9	3378	61	3314	59	4171	69	
Serotransferrin	TRFE_HUMAN	P02787	79280	Iron transport	2105	35	2260	38	30	2		1187	23	1167	23	1775	29		
Hemopexin (Beta-1B-glycoprotein)	HEMO_HUMAN	P02790	52385	Transport	491	10	633	11	74	3	293	5	167	4	312	5	32	1	
Vitamin D-binding protein	VTDB_HUMAN	P02774	52964	Transport/cell communication	469	5	712	10			835	13			452	6			
Apolipoprotein A-I	APOA1_HUMAN	P02647	30759	Cholesterol transport	462	8	422	8	124	6	28	1	177	4	373	9	333	7	
Haptoglobin	HPT_HUMAN	P00738	45861	Iron homeostasis, metabolism	310	8	261	7				98	4	37	1	193	6		
Insulin-like growth factor-binding protein 6	IBP6_HUMAN	P24592	25322	IGF binding protein	109	2	105	2			276	5			142	3			
Apolipoprotein H	APOH_HUMAN	P02749	38298	Binding neg. charged subst.	98	2	172	2			303	5			155	3			
Transthyretin	TTHY_HUMAN	P02766	15991	Hormone transport	46	2	138	5			124	2	198	3	216	3	149	2	
Hemoglobin beta chain	HBB_HUMAN	P68871	15998	Oxygen transport	44	1													
SPARC	SPRC_HUMAN	P09486	34632	Cell growth	37	1					93	3			52	1			
Collagen alpha-1(VI) chain	CO6A1_HUMAN	P12109	108529	Cell binding	37	1	40	1			60	2			87	3			
Insulin-like growth factor-binding protein 7	IBP7_HUMAN	Q16270	29130	IGF binding protein	37	1	119	2			122	3			59	1			
Tetranectin	TETN_HUMAN	P05452	22567	Binding/transport	27	1	68	2			170	4			124	2			
Plasma retinol-binding protein	RETBP_HUMAN	P02753	23010	Transport/binding			209	4			278	5			47	1			
Hemoglobin subunit alpha	HBA_HUMAN	P69905	15258	Oxygen transport			115	1											
Insulin-like growth factor-binding protein 2	IBP2_HUMAN	P18065	35138	IGF binding protein			88	2			149	4			30	1			
Lumican	LUM_HUMAN	P51884	38429	Binds to Laminin			83	2											
Protein kinase C-binding protein NELL2	NELL2_HUMAN	Q99435	91346	Binding			61	2			137	3			39	1			
Opioid-binding protein/cell adhesion molecule	OPCM_HUMAN	Q14982	38008	Opioid binding			56	1			53	1							
Apolipoprotein C-I	APOC1_HUMAN	P02654	9332	Transport			25	1											
Huntingtin-interacting protein 1-related protein	HIP1R_HUMAN	O75146	119388	Binding, stabilizing					31	2									
Apolipoprotein D	APOD_HUMAN	P05090	21276	Transport							68	2			83	1			
Afamin	AFAM_HUMAN	P43652	69069	Transport							50	1			54	1			
<i>Immune response/defense</i>																			
Ig gamma-1 chain C region	IGHG1_HUMAN	P01857	36596	Immune response	480	5	397	9					241	4			491	7	
Alpha-1-acid glycoprotein 1	A1AG1_HUMAN	P02763	23512	Acute phase response	335	4	196	4			41	1	94	2	119	2	240	3	
Alpha-1-acid glycoprotein 2	A1AG2_HUMAN	P19652	23603	Acute phase response	204	3							79	2			223	3	
Ig gamma-2 chain C region	IGHG2_HUMAN	P01859	35885	Immune response	192	2	281	9											
Ig gamma-4 chain C region	IGHG4_HUMAN	P01861	35941	Immune response	190	3	267	5					180	3			375	5	
Ig kappa chain C region	KAC_HUMAN	P01834	11773	Immune response	185	2	412	5					208	3	58	1	215	4	
Ig alpha-1 chain C region	IGHA1_HUMAN	P01876	38486	Immune response	155	3	160	3					117	3			105	3	

Table 2 (Continued)

Protein name	Uniprot entry	Uniprot Acc.	MW	Function	Intact CSF		Montage FT		Montage B		IgY-12 FT		IgY-12 B		PP-20 FT		PP-20 B	
					Score	Pep.	Score	Pep.	Score	Pep.	Score	Pep.	Score	Pep.	Score	Pep.	Score	Pep.
Alpha-1B-glycoprotein	A1BG_HUMAN	P04217	54809	Defense response	119	2	216	4			569	13			267	8		
Ig gamma-3 chain C region	IGHG3_HUMAN	P01860	32331	Immune response	86	1	180	5									125	2
Ig heavy chain V-III region BRO	HV305_HUMAN	P01766	13332	Immune response	71	1						82	1				172	2
Ig lambda chain C regions	LAC_HUMAN	P01842	11237	Immune response	33	1	55	1							27	1		
Ig alpha-2 chain C region	IGHA2_HUMAN	P01877	36508	Immune response			195	3										
Myeloid cell-spec. leu-rich glycoprotein	CD14_HUMAN	P08571	40076	Inflammatory response			101	2			82	1			72	3		
Ig heavy chain V-I region HG3	HV102_HUMAN	P01743	12946	Immune response			63	1										
Semaphorin-7A	SEM7A_HUMAN	O75326	74824	CNS immune functions			53	1			100	2						
Ig kappa chain V-III region SIE	KV302_HUMAN	P01620	11775	Immune response			49	1									33	1
Ig heavy chain V-III region WEA	HV302_HUMAN	P01763	12256	Immune response			48	1				89	1					
Ig kappa chain V-III region NG9 [Fragment]	KV303_HUMAN	P01621	10729	Immune response			44	1										
Coagulation factor XII	FA12_HUMAN	P00748	67818	Coagulation factor							54	2						
Ribonuclease K6	RNAS6_HUMAN	Q93091	17196	Defense response							30	1						
Ig heavy chain V-III region HIL	HV310_HUMAN	P01771	13566	Immune response									43	1				
<i>Complement factors</i>																		
Complement C3	CO3_HUMAN	P01024	188569	Immune response	805	14	857	22	38	3	549	13	235	7	99	3	827	17
Complement C4-A	CO4A_HUMAN	P0C0L4	194247	Complement activation	443	10	802	17			526	12			193	5	368	9
Complement factor H	CFAH_HUMAN	P08603	139070	Complement activation	177	5	140	4			29	1						
Complement factor B	CFAB_HUMAN	P00751	85533	Complement activation	135	2	285	5			500	9			127	2		
Complement component C7	CO7_HUMAN	P10643	93518	Complement activation/defense	97	1	216	4			273	4			25	1		
Complement component C9	CO9_HUMAN	P02748	63173	Complement activation	57	1	34	1	43	2	158	2			57	1		
Complement C1r	C1R_HUMAN	P00736	80174	Complement factor C1 activity	51	1	246	6			172	4						
Complement C1q subcomponent subunit B	C1QB_HUMAN	P02746	26459	Complement activation	46	1												
Complement C1q subcomponent subunit C	C1QC_HUMAN	P02747	25774	Complement activation	34	1												
Complement C2	CO2_HUMAN	P06681	83268	Complement activation	33	1												
Complement C1s subcomponent	C1S_HUMAN	P09871	76684	Complement activation							49	2						
Complement C5	CO5_HUMAN	P01031	188331	Complement activation							43	1						
<i>Metabolism/enzymes and inhibitors</i>																		
Apolipoprotein E	APOE_HUMAN	P02649	36154	Lipid metabolism	778	13	777	15	461	17	663	12	328	7	873	19	296	7
Cystatin C	CYTC_HUMAN	P01034	15799	Enzyme regulator	726	12	601	13	166	9	950	22	131	3	930	19		
Alpha-1-antitrypsin	A1AT_HUMAN	P01009	46878	Inhibitor/immune response	608	10	567	9					344	7	79	2	526	9
Alpha-2-macroglobulin	A2MG_HUMAN	P01023	164600	Inhibitor	501	10	635	14					186	6	62	2	369	9
Dickkopf-related protein 3	DKK3_HUMAN	Q9UBP4	38291	Inhibitor of Wnt signaling pathway	335	5	369	7	29	1	405	7			265	4		
Prostaglandin-H2 D-isomerase	PTGDS_HUMAN	P41222	21029	Enzyme activity	329	7	350	8	311	13	729	17	101	4	505	15	69	2
Ceruloplasmin (Ferroxidase)	CERU_HUMAN	P00450	188569	Iron transport, enzyme activity	329	7	713	14			362	9			52	2	256	6
Ectonucl. pyrophosphat./phosphodiesterase 2	ENPP2_HUMAN	Q13822	99004	Lipid metabolism	294	8	340	8			445	11			195	5		
Poly-N-acetyllactosamine extension enzyme	B3GN1_HUMAN	O43505	47119	Enzyme	272	4	283	6	40	1	251	7			115	3		

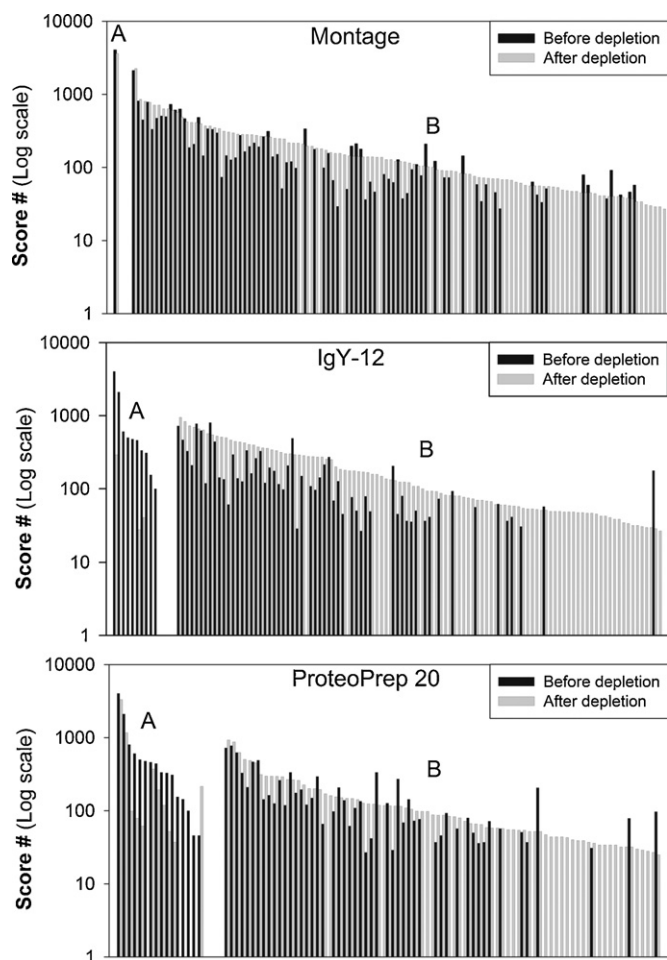
Kininogen	KNG1_HUMAN	P01042	72996	Inhibitor/inflammatory response	262	4	267	4			375	6		292	5	
Antithrombin-III	ANT3_HUMAN	P01008	52602	Serine protease inhibitor	208	5	102	3			301	7		151	4	
Apolipoprotein A-IV	APOA4_HUMAN	P06727	45399	Lipid metabolism	195	5	142	5			341	11		226	7	
Plasminogen	PLMN_HUMAN	P00747	90569	Enzyme/immune response	144	5	304	7							57	2
Ribonuclease pancreatic	RNAS1_HUMAN	P07998	17644	RNA cleavage	139	1	251	4			437	7		148	4	
CD59 glycoprotein	CD59_HUMAN	P13987	14177	Inhibitor/defense	127	2	121	2			184	3		117	2	
Superoxide dismutase	SODC_HUMAN	P00441	15936	Radical deactivation	93	1	111	1			80	1		84	1	
Phospholipid transfer protein	PLTP_HUMAN	P55058	54739	Lipid metabolism/transport	72	1	90	1				27	1	58	2	
Zinc-alpha-2-glycoprotein	ZA2G_HUMAN	P25311	33872	Lipid metabolism	66	1	156	2						171	2	
ADAM 22	ADA22_HUMAN	Q9P0K1	100433	Enzyme activity	58	1	73	1			52	1				
Ecto-ADP-ribosyltransferase 4	NAR4_HUMAN	Q93070	35878	Enzyme activity	37	1	30	1	29	1						
Angiotensinogen	ANGT_HUMAN	P01019	53154	Metabolism	36	1	140	2			108	1		65	1	
Beta-Ala-His dipeptidase	CNDP1_HUMAN	Q96KN2	56692	Enzyme activity			76	3								
Cathepsin D	CATD_HUMAN	P07339	44552	Enzyme activity			70	2								
Procollagen C-endopeptidase enhancer 1	PCOC1_HUMAN	Q15113	47972	Enzyme activity			47	2			48	2		58	2	
Insulin-like growth factor II	IGF2_HUMAN	P01344	20140	Growth promoting activity			45	1	33	1	81	2		43	1	
Glutathione S-transferase P	GSTP1_HUMAN	P09211	23356	Enzyme activity			34	1								
Inter-alpha-trypsin inhibitor heavy chain H1	ITI1_HUMAN	P19827	101389	Cell regulation			29	1						32	1	
DNA-binding protein SATB1	SATB1_HUMAN	Q01826	85957	Transcription regulation					52	3						
Nuclear factor erythroid 2-related factor 1	NF2L1_HUMAN	Q14494	84704	Transcription regulation					31	1						
TBC1 domain family member 8	TBCD8_HUMAN	Q95759	130835	Enzyme activity					30	2						
Chromodomain-helicase-DNA-binding protein 8	CHD8_HUMAN	Q9HCK8	290518	Enzyme activity					30	1						
PAP-associated domain-containing protein 5	PAPD5_HUMAN	Q8NDF8	63267	Enzyme activity					27	1						
ProSAAS	PCSK1_HUMAN	Q9UHG2	27372	Inhibitor							67	2		34	1	
Metalloproteinase inhibitor 1	TIMP1_HUMAN	P01033	23171	Inhibitor							52	2		29	1	
Peptidyl-glycine alpha-amidating monooxygenase	AMD_HUMAN	P19021	108332	Enzyme activity							50	1				
Carboxypeptidase E	CBPE_HUMAN	P16870	53151	Enzyme activity							49	1				
Extracellular superoxide dismutase	SODE_HUMAN	P08294	25851	Radical deactivation							48	1		52	2	
Cathepsin L	CATL_HUMAN	P07711	37564	Protein degradation							41	1		44	1	
Epididymal secretory protein E1	NPC2_HUMAN	P61916	16570	Lipid metabolism							34	1				
Plasma protease C1 inhibitor	IC1_HUMAN	P05155	55154	Inhibitor							30	1				
Iduronate 2-sulfatase	IDS_HUMAN	P22304	61873	Enzyme activity										55	1	
Calpain-11	CAN11_HUMAN	Q9UMQ6	80583	Enzyme activity										34	1	
Ribonuclease 4	RNAS4_HUMAN	P34096	16840	Nucleotide specificity										34	1	
Isocitrate dehydrogenase [NAD] subunit alpha	IDH3A_HUMAN	P50213	39592	Enzyme activity											32	1
Inter-alpha-trypsin inhibitor heavy chain H2	ITI2_HUMAN	P19823	106436	Transport/binding										32	1	
<i>Cell proliferation/communication/signal transduction</i>																
Calsyntenin-1	CSTN1_HUMAN	O94985	109793	Signal transduction	215	4	274	6			254	6		161	3	
Amyloid-like protein 1	APLP1_HUMAN	P51693	72176	Signal transduction	210	4	141	4	73	10	695	15		487	11	

Table 2 (Continued)

Protein name	Uniprot entry	Uniprot Acc.	MW	Function	Intact CSF		Montage FT		Montage B		IgY-12 FT		IgY-12 B		PP-20 FT		PP-20 B	
					Score	Pep.	Score	Pep.	Score	Pep.	Score	Pep.	Score	Pep.	Score	Pep.	Score	Pep.
Gelsolin	GELS.HUMAN	P06396	86043	Actin modulation	163	2	282	4			397	8			297	5	32	1
Pigment epithelium-derived factor	PEDF.HUMAN	P36955	46484	Differentiation/Inhibitor	101	2	93	1	31	2	357	6			201	3		
Fibrinogen alpha chain	FIBA.HUMAN	P02671	95656	Coagulation	100	2											39	1
Alpha-2-HS-glycoprotein	FETUA.HUMAN	P02765	39325	Promotes endocytosis	91	2	40	1										
Fibrinogen gamma chain	FIBG.HUMAN	P02679	52106	Coagulation	72	1	90	2										
Fibrinogen beta chain	FIBB.HUMAN	P02675	56577	Coagulation	63	1	140	4										
Amyloid beta A4 protein	A4.HUMAN	P05067	86943	Signal/neurite outgrowth	62	2	122	3			463	12			147	5		
Beta-2-microglobulin	B2MG.HUMAN	P61769	13715	Signal transduction	50	1	144	3			159	3			66	2		
CD44 antigen	CD44.HUMAN	P16070	81554	Mediates cell-cell interactions	46	1	37	1			180	4			87	2		
Tyrosine-protein phosphatase non-receptor type substrate 1	SHPS1.HUMAN	P78324	54813	Cell surface receptor/adhesion	45	1	70	1			49	2			98	2		
Ephrin type-A receptor 4	EPHA4.HUMAN	P54764	109860	Signal transduction	34	1	72	3										
Neurosecretory protein VGF	VGF.HUMAN	O15240	67287	Growth factor/signal transduction			38	1			73	1			40	1		
Guanine nucleotide-binding protein subunit alpha-13	GNA13.HUMAN	Q14344	44050	Signal transduction					29	1								
Low-density lipoprotein receptor-related protein 4	LRP4.HUMAN	O75096	212045	Surface receptor					28	1								
Structural/membrane associated/extracellular matrix Fibronectin	FINC.HUMAN	P02751	266034	Cell structure/communication	206	5	411	11			130	3			52	2		
Fibulin-1	FBLN1.HUMAN	P23142	77261	Extracellular matrix protein	176	5	183	6			333	7			260	6		
Neuronal cell adhesion molecule	NRCAM.HUMAN	Q92823	143894	Cell adhesion	150	3	248	6			284	7			200	4		
Neural cell adhesion mol. L1-like protein	CHL1.HUMAN	O00533	135027	Extracellular matrix protein	126	3	297	7			426	9			296	5		
EGF-containing fibulin-like extracellular matrix protein 1	FBLN3.HUMAN	Q12805	54641	Extracellular matrix protein	116	2	217	5			316	8						
Thy-1 membrane glycoprotein	THY1.HUMAN	P04216	17935	Cell-cell interaction	80	1	128	2			124	2			67	2		
Extracellular matrix protein 1	ECM1.HUMAN	Q16610	60674	Extracellular matrix protein	79	2	45	1			167	3			32	1		
Brevican core protein	PGCB.HUMAN	Q96GW7	99118	Nervous system development	77	2	105	3			176	4			98	2		
Vitronectin	VTNC.HUMAN	P04004	55069	Cell adhesion/communication	73	2	312	6			87	2			99	3		
Limbic system-associated membrane protein	LSAMP.HUMAN	Q13449	37393	Neuronal growth	69	2	128	2			200	3			109	2		
Dystroglycan	DAG1.HUMAN	Q14118	97581	Cytoskeleton receptor	63	1	56	1			61	2						
Mimecan	MIME.HUMAN	P20774	33922	Bone formation	57	1	45	1			70	2			80	2		
Neurocan core protein	CSPG3.HUMAN	O14594	142973	Neuronal adhesion neurite growth	51	1	55	2			108	3			54	1		
SPARC-like protein 1	SPRL1.HUMAN	Q14515	75216	Extracellular matrix protein	29	1	156	4			290	5			116	3		
Charged multivesicular body protein 1b	CHM1B.HUMAN	Q7LBR1	22109	Multivesicular body formation	29	1							32	1	28	1	28	1
Contactin-1	CNTN1.HUMAN	Q12860	113320	Nervous system development			149	4			176	5			88	3		
Galectin-3-binding protein	LG3BP.HUMAN	Q08380	65331	Cell adhesion			138	5			43	1			118	3		
Neuronal growth regulator 1	NEGR1.HUMAN	Q7Z3B1	38719	Cell adhesion/neuron growth			91	2			80	2						



Neural cell adhesion molecule 1, 140 kDa isoform	NCA11_HUMAN	P13591	93361	Cell adhesion	81	2				75	1			55	2			
Neurotrimin	NTRI_HUMAN	Q9P121	37971	Cell adhesion	68	1			133	2				44	1			
Collagen alpha-1(I) chain	CO1A1_HUMAN	P02452	138911	Fibril forming	67	2			47	1				44	1			
IgGfC-binding protein	FCGBP_HUMAN	Q9Y6R7	572068	Mucosal structure maintenance	41	2												
Macrophage colony-stimulating factor 1 receptor	CSF1R_HUMAN	P07333	107984	CSF-1 receptor	40	1			32	1				39	1			
Contactin-2	CNTN2_HUMAN	Q02246	113393	Axon growth/cell adhesion	29	1												
Bullous pemphigoid antigen 1, isoforms 6/9/10	BPAEA_HUMAN	O94833	590993	Cytoskeleton linker	27	1												
Transmembrane protein 169	TM169_HUMAN	Q96HH4	33611	Membrane protein					32	1								
Spectrin alpha chain, erythrocyte	SPTA1_HUMAN	P02549	279998	Cytoskeleton protein					27	1								
Neurofascin	NFASC_HUMAN	O94856	150027	Cell adhesion							92	4						
Myelin-oligodendrocyte glycoprotein	MOG_HUMAN	Q16653	28179	Myelin sheath component							58	2						
Oligodendrocyte-myelin glycoprotein	OMGP_HUMAN	P23515	49608	Cell adhesion/myelination							54	1						
Protein NOV homolog	NOV_HUMAN	P48745	39162	Cell growth regulation							47	1						
Cell adhesion molecule 3	CADM3_HUMAN	Q8N126	43300	Cell-cell adhesion							46	1						
Neural cell adhesion molecule 2	NCAM2_HUMAN	O15394	92932	Cell adhesion							39	1						
Cadherin-13	CAD13_HUMAN	P55290	78287	Cell adhesion/cell cycle							39	1						
Lethal(2) giant larvae protein homolog 1	L2GL1_HUMAN	Q15334	115042	Cytoskeleton protein							32	1						
Cell surface glycoprotein MUC18	MUC18_HUMAN	P43121	71607	Cell adhesion							31	1						
Collagen alpha-1(XVIII) chain	COIA1_HUMAN	P39060	178160	Retinal/neural tube structure											37	1		
Membrane frizzled-related protein	MFRP_HUMAN	Q9BY79	62212	Eye development											27	1		
Miscellaneous	Miscellaneous																	
Clusterin	CLUS_HUMAN	P10909	53031	Apoptosis	627	10	489	9	102	8	638	12	213	4	626	10	327	5
Prothrombin	THRB_HUMAN	P00734	71475	Acute phase response	143	4	82	2			272	7			105	3		
Kallikrein-6	KLK6_HUMAN	Q92876	26856	Enzyme activity	143	3	370	6			512	9			299	6		
Alpha-1-antichymotrypsin	AACT_HUMAN	P01011	47651	Probable inhibitor	58	1	71	2										
Histidine-rich glycoprotein	HRG_HUMAN	P04196	60510	Not listed	42	1	39	1	38	2	59	2			123	4		
Secretogranin I (Chromogranin B)	SCG1_HUMAN	P05060	78246	Precursor for active peptides	42	1	56	1			93	2						
Major prion protein	PRIO_HUMAN	P04156	27661	Not listed	31	1					55	2			36	1		
AMBP protein	AMBP_HUMAN	P02760	38999	Complex forming			57	1			77	2						
Leucine-rich alpha-2-glycoprotein	A2GL_HUMAN	P02750	38178	Not listed			54	2										
Voltage-dependent calcium channel subunit alpha-2/delta-1	CAC2D_HUMAN	P54289	123183	Calcium channel protein			47	1			62	3						
Immunoglobulin superfamily member 8	IGSF8_HUMAN	Q969P0	65034	Multiple enzymatic functions			41	1			27	1			25	1		
Secretogranin-3	SCG3_HUMAN	Q8WXD2	53005	Not listed			31	1										
THUMP domain-containing protein 1	THUM1_HUMAN	Q9NXG2	39315	Unambiguous					34	1								
Protein FAM3C	FAM3C_HUMAN	Q92520	24680	Not listed							70	3			34	1		
Retinoic acid receptor responder protein 2	RARR2_HUMAN	Q99969	18618	Calcium channel protein							61	2						
Cartilage acidic protein 1	CRAC1_HUMAN	Q9NQ79	71421	Not listed							50	1						
Ribonuclease T2	RNT2_HUMAN	O00584	29481	Not listed							35	1						



**Fig. 3.** MASCOT scores (log<sub>10</sub>) for significantly matched (MudPIT 95% ( $p \leq 0.05$ ) confidence) proteins before (black bars) and after (grey bars) sample preparation of 1 mL CSF by the three different spin column kits. A: High abundant proteins targeted for removal, B: remaining medium–low abundant proteins.

abundant proteins are dramatically increased even though the targeted subtraction proteins are not removed but, as for the Montage column, merely reduced in concentration. The greatest reduction of the high abundant proteins was observed for the ProteomeLab IgY-12 spin column where the MASCOT scores for the majority of the proteins were completely diminished and for the remaining reduced by up to 17 times. Additionally, MASCOT scores for the medium and low abundant proteins were increased by more than 10 times or, for most low abundant proteins, only identified after the removal of the high abundant proteins. Although the removal or reduction of the high abundant proteins in CSF leads to an increased number of medium–low abundant proteins identified with increased MASCOT scores, it is also important to be aware of the possibilities of co-removal of low abundant proteins. Proteins identified in each corresponding bound fraction are listed in Table 2. Both the ProteomeLab IgY-12 and ProteoPrep 20 spin columns show very high specificity and low non-specific co-removal, while the entirely affinity based Montage column has a higher degree of non-specific protein subtraction. The ProteomeLab IgY-12 bound fraction contains 10 out of the 12 targeted proteins, only Apolipoprotein A-II and Fibrinogen are not detected. However, human CSF should normally contain moderate concentrations of Fibrinogen, which explains the lack of identification. The subtraction column has primarily been developed for human plasma samples and is therefore not completely optimal for human CSF. The bound fraction from the ProteomeLab IgY-12 column contains

9 non-targeted proteins. Nonetheless, most of these proteins, such as Prostaglandin-H2 D-isomerase (beta-trace) and Transthyretin (prealbumin) are considered high abundant in CSF and are therefore likely to be present in the bound fraction due to non-specific binding. The presence of these non-targeted proteins in the bound fraction will, however, have implications on any quantitative studies performed on the flow through fractions. These proteins should not be quantitatively evaluated in the FT fraction, since their concentrations are questionable. Thus, it is clearly of interest to analyze the protein content in the bound fractions when fractionating the sample and exclude, or at least be very cautious in including the identified proteins in any comparative studies. The bound fraction for the ProteoPrep 20 spin column contained 17 out of the 20 targeted proteins and 6 non-targeted. The targeted proteins missing were Apolipoprotein A-II, Apolipoprotein B and Complement factor C1q. Again, this column was designed for the preparation of human plasma. Apolipoprotein B is not high abundant in human CSF. In fact, it can be used as an indicator for blood contamination in CSF [2] and the absence of Apolipoprotein B in the bound fraction is therefore not surprising. The bound fraction for the Montage spin column contained 28 proteins, which clearly demonstrates the non-specific co-removal of proteins due to the albumin sponge effect. It can also be explained by the fact that this column is purely affinity based and therefore has a tendency to bind other non-targeted proteins. Again, this non-specific removal of the proteins will have implications on any quantitative analysis on the remaining protein fractions in the corresponding FT sample.

### 3.3. Column reproducibility and iTRAQ labeling

Based on the number of proteins identified, in combination with the specificity of protein removal, the ProteomeLab IgY-12 spin column was further evaluated regarding reproducibility and compatibility for LC–MS/MS quantification using stable isotopic labeling. Differential diagnosis based on comparative proteomic studies with quantitative mass spectrometry has seen a major breakthrough in recent years and the use of isotope coded tags is specifically popular. One of the most accepted approaches is the isobaric tags for relative and absolute quantification [38] that enables multiplexed quantitative analysis of up to eight samples simultaneously. The reproducibility and use of the ProteomeLab IgY-12 spin column on human CSF was evaluated iTRAQ labeling and quantification. This approach will estimate the reproducibility of the combination of the high abundant protein removal, the iTRAQ labeling and the MS/MS detection and thereby mimic the experimental conditions for a screening study of clinically relevant samples. The obtained iTRAQ ratios are plotted in Fig. 4A (99% MudPIT confidence scoring) and Fig. 4B (95% MudPIT confidence scoring). In the ideal case, the expected iTRAQ ratios would be 1:1:1:1. The iTRAQ manufacturer (Applied) states an estimated labeling and MS/MS variation of roughly 20%. On normalized values this would imply that ratios between 1.2 and 0.83 are considered as “no change” or within the expected experimental variation. Abdi et al. [2] have previously stated that iTRAQ ratios greater than 20% but less than 50% to have an unlikely and uncertain significance in a quantitative study of human CSF. Therefore, changes in the protein expression in the CSF have to yield iTRAQ ratios increased or decreased by 50% to be considered significant. Consequently, a normalized ratio greater than 1.5 should be considered as a significantly up-regulated protein and a normalized value smaller than 0.67 should be considered as a significantly down-regulated protein. Almost all iTRAQ ratios plotted in Fig. 4A and B are within the boundaries to be considered “no change”. Since all ratios are expected to be 1:1:1:1, the average ratio values and relative standard deviation (R.S.D.) can be calculated for the entire method. For the 99% MudPIT MASCOT scoring the average 115/114, 116/114

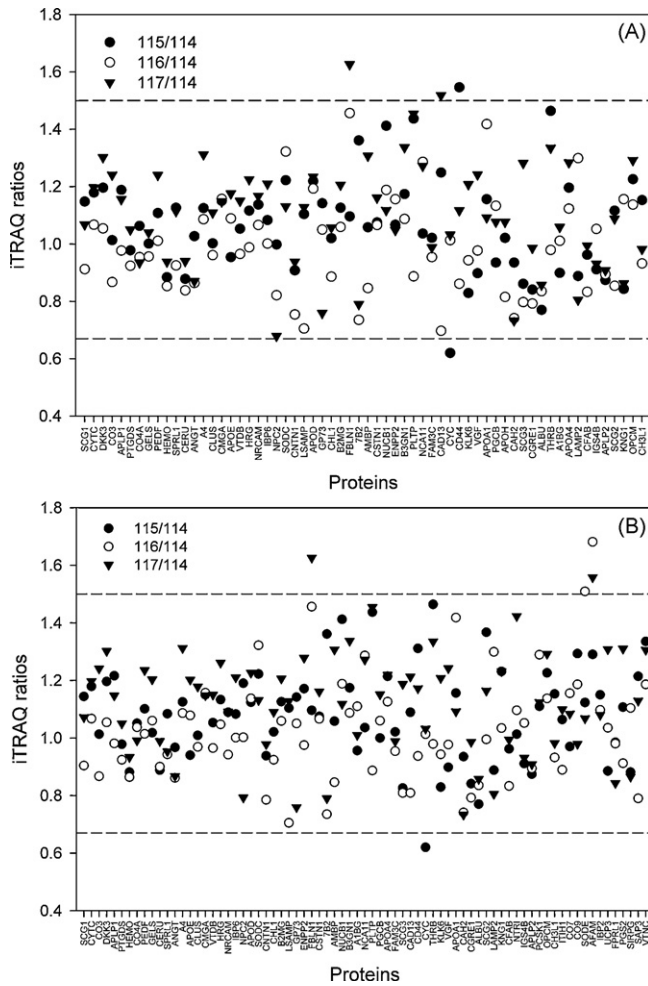


**Fig. 4.** (A and B) iTRAQ 4-plex ratios for the significantly matched proteins in CSF after ProteomeLab IgY-12 processing with A: 99% MudPIT confidence scoring and B: 95% MudPIT confidence scoring. All iTRAQ ratios are expected to be 1:1:1:1. The dashed lines represent iTRAQ ratios of 1.5 and 0.67, which corresponds to significant up and down-regulation respectively according to Abdi et al. [2].

and 117/114 ratios were found to be 1.07, 0.99 and 1.11 with R.S.D. values of 16.1%, 16.9% and 16.9%, respectively. On a 95% MudPIT MASCOT scoring level the average 115/114, 116/114 and 117/114 ratios were found to be 1.08, 1.02 and 1.12 with R.S.D. values of 14.9%, 17.5% and 16.0%, respectively. The obtained average and R.S.D. values are well within the 20% variation stated for the labeling alone. This indicates that the high abundant protein subtraction with the ProteomeLab IgY-12 spin column followed by iTRAQ labeling, nanoLC separation and MALDI-TOF/TOF-MS detection yields very reproducible results. However, looking further on individual protein levels one can notice that a few proteins actually show up- and down-regulated levels both on a 99% and 95% MudPIT MASCOT scoring level. On the 99% level, Fibulin-1 and Cadherin-13 had iTRAQ 117/114 ratios greater than 1.5 and the 115/114 ratios for Cytochrome C and CD 44 antigen were less than 0.67 and greater than 1.5, respectively. On the 95% level, the same results were obtained for Fibulin-1 and Cytochrome C but not the other proteins. Meanwhile, the 116/114 ratio for Extracellular superoxide dismutase was greater than 1.5, which was also the case for both the 116/114 and 117/114 ratios for Afamin. Statistically, a few outlier results are to be expected. However, these outliers accentuate the need to have an experimental design that includes numerous biological and technical replicates when performing biomarker screening studies. Trends of up- and

down-regulations must be consistent throughout all biological and technical replicates to be considered as potential biomarkers. For instance, both Cytochrome C and Extracellular superoxide dismutase that by chance and wrongfully showed significant changes have extensively been reported to be altered in numerous diseases. Finally, as stated previously, it is believed that many potential biomarkers secreted in biofluids would be present at very low concentrations. This will have implications on any quantitative study. These proteins are likely to be identified by only 1–2 peptides at low MS intensities, which in turn give very poor data for any statistics or quantification.

#### 4. Conclusions

In this study, the performance of three different affinity/antibody protein subtraction kits for the preparation of human CSF was compared. A rather large CSF volume, up to 1 mL, could be processed with all three columns with retained partitioning efficiency. All three columns also yielded an increased number of proteins identified as well as increased MASCOT ionscores for the remaining medium–low abundant proteins. The analysis of the protein content of the bound proteins showed varying degrees of non-targeted protein removal. It is of interest to analyze the bound fractions as non-targeted protein removal will influence any quantitative proteomic studies. These proteins should be excluded in the study, unless they exclusively can be quantified in the bound protein fractions. The reproducibility for the overall procedure of sample processing and quantitative MS/MS analysis was investigated for the ProteomeLab IgY-12 spin column in combination with iTRAQ labeling. The overall process of protein removal, isotopic labeling and MS/MS analysis was very reproducible and the overall variation was less than 17.5%, making this approach suitable for quantitative comparisons of CSF samples. However, the experimental data support previous statements that limits for up and down-regulation in CSF should be set to at least 50% change and be consistent in numerous biological replicates.

#### Acknowledgements

This research was supported by Uppsala Berzelii Technology Center for Neurodiagnostics, with financing from the Swedish Governmental Agency for Innovation Systems and the Swedish Research Council Grant numbers P29797-1 and 621-2008-3562. Andreas Dahlin is acknowledged for assistance with Fig. 1.

#### References

- [1] J. Zhang, D.R. Goodlett, T.J. Montine, J. Alzheimers Dis. 8 (2005) 377.
- [2] F. Abdi, J.F. Quinn, J. Jankovic, M. McIntosh, J.B. Leverenz, E. Peskind, R. Nixon, J. Nutt, K. Chung, C. Zabetian, A. Samii, M. Lin, S. Hattan, C. Pan, Y. Wang, J. Jin, D. Zhu, G.J. Li, Y. Liu, D. Waichunas, T.J. Montine, J. Zhang, J. Alzheimers Dis. 9 (2006) 293.
- [3] W.M. Caudle, S. Pan, M. Shi, T. Quinn, J. Hoekstra, R.P. Beyer, T.J. Montine, J. Zhang, Proteomics Clin. Appl. 2 (2008) 1484.
- [4] J. Zhang, C.D. Keene, C. Pan, K.S. Montine, T.J. Montine, J. Neuropathol. Exp. Neurol. 67 (2008) 923.
- [5] S. Roche, A. Gabelle, S. Lehmann, Proteomics Clin. Appl. 2 (2008) 428.
- [6] M. Shi, W.M. Caudle, J. Zhang, Neurobiol. Dis. 35 (2009) 157.
- [7] S. Jesse, P. Steinacker, S. Lehnert, F. Gillardon, B. Hengerer, M. Otto, CNS Neurosci. Ther. 15 (2009) 157.
- [8] R. Craig-Schapiro, A.M. Fagan, D.M. Holtzman, Neurobiol. Dis. 35 (2009) 128.
- [9] A. Westman-Brinkmalm, U. Ruetschi, E. Portelius, U. Andreasson, G. Brinkmalm, G. Karlsson, S. Hansson, H. Zetterberg, K. Blennow, Front. Biosci. 14 (2009) 1793.
- [10] H. Reiber, J.B. Peter, J. Neurol. Sci. 184 (2001) 101.
- [11] S. Hu, J.A. Loo, D.T. Wong, Proteomics 6 (2006) 6326.
- [12] S.M. Ahn, R.J. Simpson, Proteomics Clin. Appl. 1 (2007) 1004.
- [13] J. Zhang, D.R. Goodlett, E.R. Peskind, J.F. Quinn, Z. Yong, W. Qin, C. Pan, E. Yi, J. Eng, R.H. Aebersold, T.J. Montine, Neurobiol. Aging 26 (2005) 207.
- [14] J.P. Noben, D. Dumont, N. Kwasnikowska, P. Verhaert, V. Somers, R. Hupperts, P. Stinissen, J. Robben, J. Proteome Res. 5 (2006) 1647.
- [15] K.S. Shores, D.R. Knapp, J. Proteome Res. 6 (2007) 3739.

- [16] R. Siegmund, M. Kiehnopf, T. Deufel, *Clin. Biochem.* 42 (2009) 1136.
- [17] P. Davidsson, L. Paulson, C. Hesse, K. Blennow, C.L. Nilsson, *Proteomics* 1 (2001) 444.
- [18] P. Davidsson, S. Folkesson, M. Christiansson, M. Lindbjer, B. Dellheden, K. Blennow, A. Westman-Brinkmalm, *Rapid Commun. Mass Spectrom.* 16 (2002) 2083.
- [19] L.N. Waller, K. Shores, D.R. Knapp, *J. Proteome Res.* 7 (2008) 4577.
- [20] X.L. Yuan, D.M. Desiderio, *Proteomics* 5 (2005) 541.
- [21] K.S. Shores, D.G. Udugamasooriya, T. Kodadek, D.R. Knapp, *J. Proteome Res.* 7 (2008) 1922.
- [22] B.N. Hammack, G.P. Owens, M.P. Burgoon, D.H. Gilden, *Mult. Scler.* 9 (2003) 472.
- [23] G. Maccarrone, D. Milfay, I. Birg, M. Rosenhagen, F. Holsboer, R. Grimm, J. Bailey, N. Zolotarjova, C.W. Turck, *Electrophoresis* 25 (2004) 2402.
- [24] M. Ramstrom, C. Hagman, J.K. Mitchell, P.J. Derrick, P. Hakansson, J. Bergquist, *J. Proteome Res.* 4 (2005) 410.
- [25] M. Ramstrom, A. Zuberovic, C. Gronwall, J. Hanrieder, J. Bergquist, S. Hober, *Biotechnol. Appl. Biochem.* 52 (2009) 159.
- [26] E. Mouton-Barbosa, F. Roux-Dalvai, D. Bouyssié, F. Berger, E. Schmidt, P.G. Righetti, L. Guerrier, E. Boschetti, O. Burlet-Schiltz, B. Monsarrat, A. Gonzalez de Peredo, *Mol. Cell. Proteomics*, Published online January 21st, 2010, doi:10.1074/mcp.M900513-MCP200.
- [27] B.R. Wenner, M.A. Lovell, B.C. Lynn, *J. Proteome Res.* 3 (2004) 97.
- [28] Y. Hu, J.P. Malone, A.M. Fagan, R.R. Townsend, D.M. Holtzman, *Mol. Cell. Proteomics* 4 (2005) 2000.
- [29] Y. Ogata, M.C. Charlesworth, D.C. Muddiman, *J. Proteome Res.* 4 (2005) 837.
- [30] J.A. Burgess, P. Lescuyer, A. Hainard, P.R. Burkhard, N. Turck, P. Michel, J.S. Rossier, F. Reymond, D.F. Hochstrasser, J.C. Sanchez, *J. Proteome Res.* 5 (2006) 1674.
- [31] Y. Hu, J.S.K. Kauwe, J. Gross, N.J. Cairns, A.M. Goate, A.M. Fagan, R.R. Townsend, D.M. Holtzman, *Proteomics Clin. Appl.* 1 (2007) 1373.
- [32] Y. Ogata, M.C. Charlesworth, L. Higgins, B.M. Keegan, S. Vernino, D.C. Muddiman, *Proteomics* 7 (2007) 3726.
- [33] L. Dayon, A. Hainard, V. Licker, N. Turck, K. Kuhn, D.F. Hochstrasser, P.R. Burkhard, J.C. Sanchez, *Anal. Chem.* 80 (2008) 2921.
- [34] A. Zuberovic, J. Hanrieder, U. Hellman, J. Bergquist, M. Wetterhall, *Eur. J. Mass Spectrom.* 14 (2008) 249.
- [35] E. Thouvenot, S. Urbach, C. Dantec, J. Poncet, M. Seveno, E. Demettré, P. Jouin, J. Touchon, J. Bockaert, P. Marin, *J. Proteome Res.* 7 (2008) 4409.
- [36] J. Granger, J. Siddiqui, S. Copeland, D. Remick, *Proteomics* 5 (2005) 4713.
- [37] R.L. Gundry, Q. Fu, C.A. Jelinek, J.E. Van Eyk, R.J. Cotter, *Proteomics Clin. Appl.* 1 (2007) 73.
- [38] T. Hunt, Y. Huang, P. Ross, S. Pillai, S. Purkayastha, D. Pappin, *Mol. Cell. Proteomics* 3 (2004) S286.
- [39] J. Bergquist, M. Palmblad, M. Wetterhall, P. Hakansson, K.E. Markides, *Mass Spectrom. Rev.* 21 (2002) 2.
- [40] J. Hanrieder, M. Wetterhall, P. Enblad, L. Hillered, J. Bergquist, *J. Neurosci. Methods* 177 (2009) 469.